Provided for non-commercial research and education use.
Not for reproduction, distribution or commercial use.

VOLUME 238 (10) OCTOBER 2008 ISSN 0029-5493

Nuclear Engineering and Design

An International Journal devoted to all aspects of Nuclear Fission Energy

Editor-in-Chief: Yassin Hassan
Editors: Jason Chao
Borut Mavko
Dominique Bestion

CONTENTS

Engineering Mechanics
Early-age behaviour of concrete nuclear containments
F. Benboudjema and J.M. Torrenti 2495
Modelling of fluidelastic vibrations of heat exchanger tubes with loose supports
M. Hassan and M. Hayder 2507

Materials Engineering
Critical impact energy for the perforation of metallic plates
S.Y. Aly and Q.M. Li 2521
Electroless nickel-plating for the PWSCC mitigation of nickel-base alloys in nuclear power plants
J.H. Kim and I.S. Hwang 2529
Hydrogen influence on mechanical and fracture mechanics characteristics of zirconium Zr–2.5Nb alloy at ambient and elevated temperatures
M. Daunys, R. Dundulis, A. Grybenas and P. Krasauskas 2536

Reactor Engineering
Implementation of a strainer model for calculating the pressure drop across beds of compressible, fibrous materials
A. Grahn, E. Krepper, S. Alt and W. Kästner 2546
A study on evaluating a passive autocatalytic recombiner PAR-system in the PWR large-dry containment
J. Deng and X.W. Cao 2554
Analysis of a loss of residual heat removal system during mid-loop conditions at PKL facility using RELAP5/Mod3.3
S. Carlos, J.E. Villanueva, S. Martorell and V. Serradell 2561
One- and two-dimensional standing pressure waves and one-dimensional travelling pulses using the US-NRC nuclear systems analysis code TRACE
W. Barten, A. Manera and R. Macian-Juan 2568
Reactivity feedback coefficients of a material test research reactor fueled with high-density U_3Si_2 dispersion fuels
F. Muhammad and A. Majid 2583
Mesh generation technology for nuclear reactor simulation; barriers and opportunities
G. Hansen and S. Owen 2590

Fuel Engineering
Development of an advanced PWR fuel for OPR1000s in Korea
K.-T. Kim and J.-M. Suh 2606

Reactor Components
Development of a pump performance model for an integral effect test facility
K.-Y. Choi, Y.-S. Kim, S.-J. Yi and W.-P. Baek 2614

(Contents continued on back cover)

Available online at
ScienceDirect
www.sciencedirect.com

Affiliated with the European Nuclear Society (ENS) and with the International Association for Structural Mechanics in Reactor Technology, e.V. (IASMiRT)

This article appeared in a journal published by Elsevier. The attached copy is furnished to the author for internal non-commercial research and education use, including for instruction at the authors institution and sharing with colleagues.

Other uses, including reproduction and distribution, or selling or licensing copies, or posting to personal, institutional or third party websites are prohibited.

In most cases authors are permitted to post their version of the article (e.g. in Word or Tex form) to their personal website or institutional repository. Authors requiring further information regarding Elsevier's archiving and manuscript policies are encouraged to visit:

http://www.elsevier.com/copyright

Author's personal copy

Nuclear Engineering and Design 238 (2008) 2779–2791

Contents lists available at ScienceDirect

Nuclear Engineering and Design

journal homepage: www.elsevier.com/locate/nucengdes

Modeling, analysis and prediction of neutron emission spectra from acoustic cavitation bubble fusion experiments

R.P. Taleyarkhan [a,*], J. Lapinskas [a], Y. Xu [a], J.S. Cho [b], R.C. Block [c], R.T. Lahey Jr [c], R.I. Nigmatulin [d]

[a] Purdue University, West Lafayette, IN 47907, USA
[b] FNC Tech. Locn., Seoul National University, South Korea
[c] Rensselaer Polytechnic Institute, Troy, NY 12180, USA
[d] Russian Academy of Sciences, Moscow, Russia

ARTICLE INFO

Article history:
Received 29 December 2007
Received in revised form 4 June 2008
Accepted 7 June 2008

ABSTRACT

Self-nucleated and external neutron nucleated acoustic (bubble fusion) cavitation experiments have been modeled and analyzed for neutron spectral characteristics at the detector locations for all separate successful published bubble fusion studies. Our predictive approach was first calibrated and validated against the measured neutron spectrum emitted from a spontaneous fission source (^{252}Cf), from a Pu–Be source and from an accelerator-based monoenergetic 14.1 MeV neutrons, respectively. Three-dimensional Monte-Carlo neutron transport calculations of 2.45 MeV neutrons from imploding bubbles were conducted, using the well-known MCNP5 transport code, for the published original experimental studies of Taleyarkhan et al. [Taleyarkhan, et al., 2002. Science 295, 1868; Taleyarkhan, et al., 2004. Phys. Rev. E 69, 036109; Taleyarkhan, et al., 2006a. PRL 96, 034301; Taleyarkhan, et al., 2006b. PRL 97, 149404] as also the successful confirmation studies of Xu et al. [Xu, Y., et al., 2005. Nuclear Eng. Des. 235, 1317–1324], Forringer et al. [Forringer, E., et al., 2006a. Transaction on American Nuclear Society Conference, vol. 95, Albuquerque, NM, USA, November 15, 2006, p. 736; Forringer, E., et al., 2006b. Proceedings of the International Conference on Fusion Energy, Albuquerque, NM, USA, November 14, 2006] and Bugg [Bugg, W., 2006. Report on Activities on June 2006 Visit, Report to Purdue University, June 9, 2006]. NE-213 liquid scintillation (LS) detector response was calculated using the SCINFUL code. These were cross-checked using a separate independent approach involving weighting and convoluting MCNP5 predictions with published experimentally measured NE-213 detector neutron response curves for monoenergetic neutrons at various energies. The impact of neutron pulse-pileup during bubble fusion was verified and estimated with pulsed neutron generator based experiments and first-principle calculations. Results of modeling-cum-experimentation were found to be consistent with published experimentally observed neutron spectra for 2.45 MeV neutron emissions during acoustic cavitation (bubble) fusion experimental conditions with and without ice-pack (thermal) shielding. Calculated neutron spectra with the inclusion of ice-pack shielding are consistent with the published spectra from experiments of Taleyarkhan et al. [Taleyarkhan, et al., 2006a. PRL 96, 034301] and Xu et al. [Xu, Y., et al., 2005. Nuclear Eng. Des. 235, 1317–1324] where ice-pack shielding was present, whereas without ice-pack shielding the calculated neutron spectrum is consistent with the experimentally observed neutron spectra of Taleyarkhan et al. [Taleyarkhan, et al., 2002. Science 295, 1868; Taleyarkhan, et al., 2004. Phys. Rev. E 69, 036109] and Forringer et al. [Forringer, E., et al., 2006a. Transaction on American Nuclear Society Conference, vol. 95, Albuquerque, NM, USA, November 15, 2006, p. 736; Forringer, E., et al., 2006b. Proceedings of the International Conference on Fusion Energy, Albuquerque, NM, USA, November 14, 2006] and also that from GEANT computer code [Agostinelli, S., et al., 2003. Nuclear Instrum. Methods Phys. Res. A 506, 250–303] predictions [Naranjo, B., 2006. PRL 97 (October), 149403] in which ice shielding was also absent.

The results of this archive confirm for the record that the confusion and controversies caused from past reports [Reich, E., 2006. Nature (March) 060306. news@nature.com; Naranjo, B., 2006. PRL, 97

Abbreviations: Cf, californium; Ci, Curie; D, deuterium; GEANT, a Monte-Carlo nuclear particle interaction code system; n, neutron; MCNP, Monte-Carlo N-particle computer code; NE-213, trademark of scintillation liquid from Nuclear Enterprises Inc.; LS, liquid scintillation; PNG, pulse neutron generator; PRE, proton recoil edge; PSD, pulse-shape discrimination; Pu–Be, plutonium–beryllium; SCINFUL, scintillator full response computer code; T, tritium; UN, uranyl nitrate; γ, gamma photon.

* Corresponding author.
E-mail address: rusi@purdue.edu (R.P. Taleyarkhan).

0029-5493/$ – see front matter © 2008 Elsevier B.V. All rights reserved.
doi:10.1016/j.nucengdes.2008.06.007

Author's personal copy

(October) 149403] have resulted from their neglect of important details of bubble fusion experiments. Results from this paper demonstrate that ice-pack shielding between the detector and the fusion neutron source, gamma photon leakage and neutron pulse-pileup due to picosecond duration neutron pulse emission effects play important roles in affecting the spectra of neutrons from acoustic inertial confinement thermonuclear fusion experiments.

© 2008 Elsevier B.V. All rights reserved.

1. Introduction

In 2006, evidence was presented for a unique, new stand-alone acoustic inertial confinement fusion device that was successfully tested and results published (Taleyarkhan et al., 2006a). Those experiments were conducted with four different liquid types in which bubbles were nucleated without the use of external neutron sources. Four independent detector systems were used [a neutron track plastic detector to provide unambiguous visible records for fast neutrons, a LiI thermal neutron detector, a NE-213-type liquid scintillation (LS) detector, and a NaI gamma (γ) ray detector]. All detector systems measured statistically significant (from 6 to 20+ standard deviations) nuclear emissions for experiments with deuterated benzene and acetone mixtures but not for experiments with heavy water, a finding which validated theoretical predictions (Nigmatulin et al., 2005) of our simulations of the implosion dynamics which indicated that heavy water would not be a good choice for attaining thermonuclear fusion in imploding bubbles. The measured neutron energies from bubble fusion experiments were, as expected, substantially $\leq$2.45 MeV. Control experiments did not result in statistically significant neutron or γ ray emissions. These observations of neutron emissions in self-nucleated experiments with deuterated benzene–acetone mixtures but not for the controls (i.e., non-deuterated mixtures) have been successfully confirmed (Forringer et al., 2006a,b; Bugg, 2006). In the studies of Forringer et al. and Bugg, the experimental configurations they used were different from that used by Taleyarkhan et al. (2006a,b). The two experimental configurations are shown in Fig. 1a and b . As noted therein, a principle distinguishing factor between the two configurations is the presence or absence of ~3 cm of ice-pack materials acting as thermal shielding around the test cell enclosure. Whereas, in the reported experimental systems of Taleyarkhan et al. (2002, 2004, 2006a,b) the ice-pack shielding was required and present, the same was not true in the experiments conducted by Forringer et al. (2006a,b) and Bugg (2006).

The results of Taleyarkhan et al. (2006a) using the LS detector system offered the highest level of statistical significance of above 17 standard deviations (S.D.). Because of the presence of intervening ice-pack shielding, the published neutron spectrum (Taleyarkhan et al., 2006a) incorporated characteristics that were different from the shape of the neutron spectrum for a monoenergetic 2.45 MeV neutron emanating from the test cell without having to interact with ice-pack shielding. A qualitative discussion was provided (Taleyarkhan et al., 2006b) in response to questions and comments raised from code calculations for the presumed geometric configuration by Naranjo (2006) of the University of California at Los Angeles (UCLA). Unfortunately, the UCLA predictions were made for an incorrectly presumed experimental configuration (e.g., with no ice-packs) and would actually be more applicable for comparisons with the published measured neutron spectra of Forringer et al. (2006a,b) and Taleyarkhan et al. (2002, 2004) rather than those of Taleyarkhan et al. (2006a). Nevertheless, these faulty simulations seeded and caused considerable controversy and confusion (Reich, 2006; Naranjo, 2006).

In 2002 and 2004, evidence was first presented for the neutron spectrum measured during external neutron-based acoustic cavitation experiments (Taleyarkhan et al., 2002, 2004). In these experiments nucleation of bubbles in pure deuterated acetone (C_3D_6O) was achieved using a 14.1 MeV pulse neutron generator (PNG). The test geometry for this study is shown in Fig. 1d. Although the enclosure is similar to that for Fig. 1a, the LS detector was positioned to be within the enclosure as shown with no intervening ice-pack materials. The results of the 2004 studies reported by Taleyarkhan et al. (2004) were successfully confirmed in studies reported by Xu et al. (2005) in which they used a different experimental enclosure type as shown in Fig. 1c, and the bubble nucleation was conducted using randomly emitted neutrons from an isotope source. However, as for the self-nucleation bubble fusion reports of Taleyarkhan et al. (2006a,b), in the Xu et al. (2005) studies, their LS detector was also positioned outside the freezer, and as such, a ~3–4 cm of ice layer was also present between the test cell and the LS detector.

The purpose of this paper is to present a comprehensive unifying study for all the reported successful bubble fusion studies with the goal to remedy the unfortunate controversies and confusion resulting from the misguided simulations for incorrect experimental configurations as reported in the literature (Reich, 2006; Naranjo, 2006), as well as due to the omission of important effects such as pulse-pileup and gamma photon leakage. For completeness, we have conducted simulations of successful published studies not only for the self-nucleation experiments, but also, for the external neutron-based experiments.

Questions have also been raised (Reich, 2006) concerning the detection of neutron counts in channels higher than the 2.45 MeV proton recoil edge (PRE). The present paper includes results of analyses, backed up with experimental evidence, for clarifying the principle mechanisms concerning such occurrence for bubble fusion experiments.

2. Two independent modeling-simulation approaches

In order to evaluate the relative effects on the expected 2.45 MeV spectrum with and without ice-pack shielding we conducted assessments with two independent methods to obtain cross-checks and better confidence for the validity of our predictions. The first approach was to establish a simulation platform similar to that used by UCLA in which results of three-dimensional neutron transport from within the test cell were derived using the USDOE's code system MCNP5 (MCNP, 2003) at the location of the LS detector. This down scattered neutron flux profile was next combined with the USDOE's *Scintillator Full* (SCINFUL) response Monte-Carlo based code system (Dickens, 1988). SCINFUL was developed specifically for predicting the response function of neutron interactions with NE-213 detectors. The second approach we developed was to act as a cross-check to the MCNP5–SCINFUL predictions. It involves directly combining the neutron emission spectra emanating from the experimental system (as derived from MCNP5 simulations) with the published (i.e., directly measured) neutron energy-related pulse-height spectra for an actual 5 cm × 5 cm sized NE-213 detector (viz., of the same size and type as used by Taleyarkhan et al., 2002, 2004, 2006a,b; Xu et al., 2005; also by Forringer et al., 2006a,b). Predictions from both approaches could then be compared with the various published bubble fusion experimental data.

Author's personal copy

2.1. Calibration-benchmarking of LS detector with prediction methodology

The SCINFUL code requires the user to provide to it the incoming neutron energy spectrum (e.g., from a known source of neutrons of various energies). A known source could be from a National Institute of Standards and Technology (NIST)-certified isotope source or from an accelerator-based system. Alternately, it could be the prediction from a well-characterized nuclear particle transport code such as MCNP5. SCINFUL utilizes Monte-Carlo techniques and has itself been extensively benchmarked by the developers against a variety of experimental databases for its ability to predict the overall response of a NE-213 LS detector system to incoming neutrons over the energy range 0.5–80 MeV. A known shortcoming is associated with the PRE where detector resolution issues can lead to smearing-related extension of counts to higher channels in an actual detector system but this is not possible to model theoretically since it involves intricacies of individual detector construction and multidimensional issues. In order to gain confidence in the prediction methodology employed for this study it was decided to ourselves calibrate the SCINFUL code predictions for our laboratory's 5 cm × 5 cm NE-213 LS detector using the electronic component train and settings for the published bubble fusion experimental spectra. The comparisons were made for three different neutron sources. The first two were NIST-certified isotope-based neutron-gamma sources: (1) 1 Ci, Pu–Be source emitting ~2×10^6 n/s; (2) ~0.1 mCi, ^{252}Cf source emitting ~10^5 n/s. The second type of neutron source produced 14.1 MeV monoenergetic neutrons from an accelerator device commonly called a PNG and is based on D–T interactions. The emission rate was about 5×10^5 n/s. The NE-213 LS detector was placed ~30 cm from each of these sources and the spectra were obtained with and without

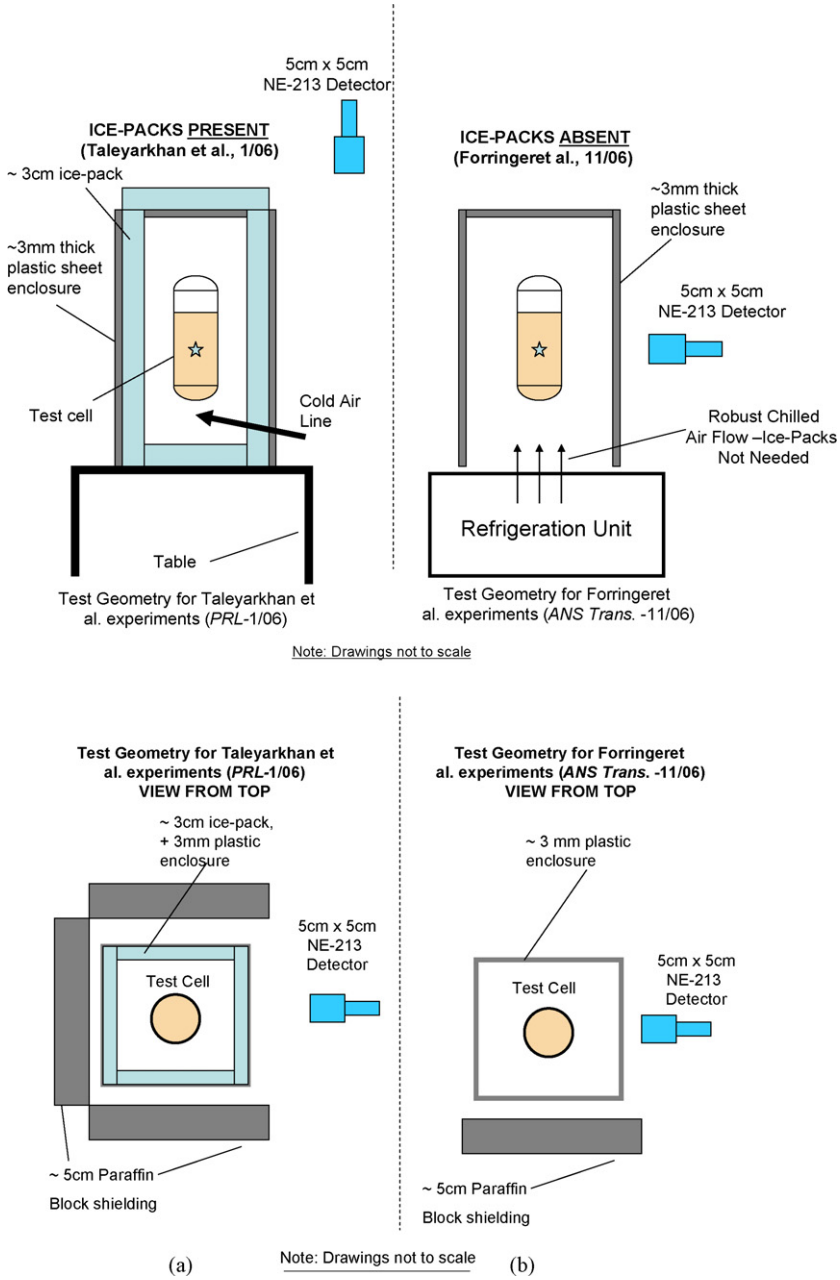

Fig. 1. Experimental geometries of (a) Taleyarkhan et al. (2006a,b) (b) Forringer et al. (2006a,b) (c) Xu et al. (2005) and (d) Taleyarkhan et al. (2002, 2004).

Author's personal copy

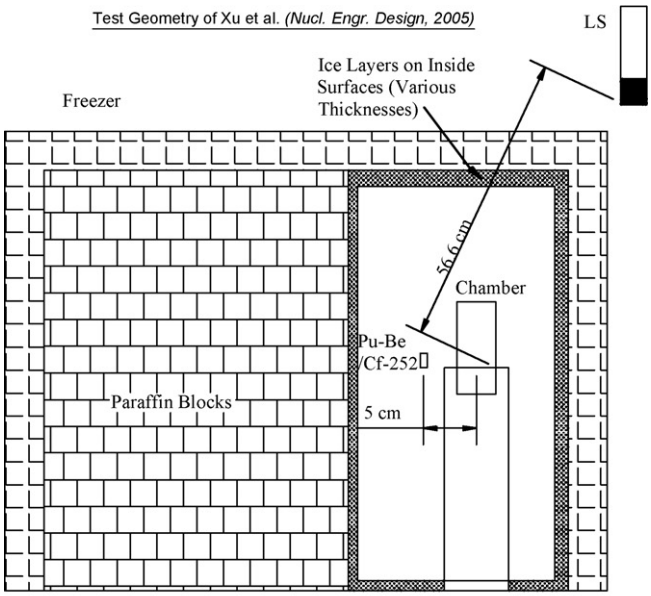

(1c) – Xu et al. (2005)

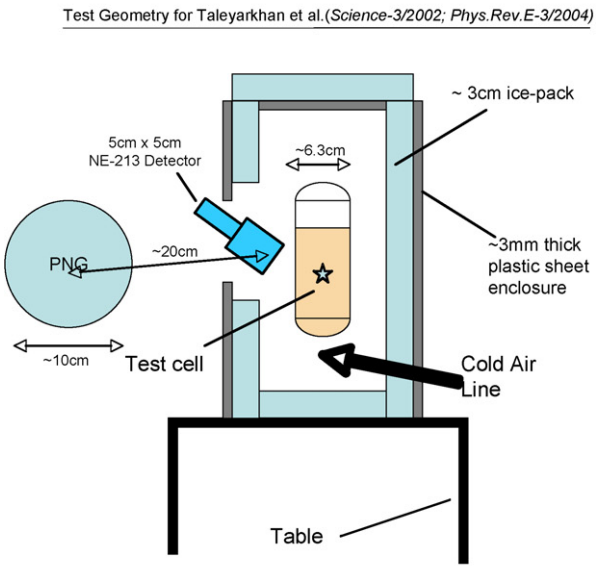

(1d) – Taleyarkhan et al. (2002, 2004)

Fig. 1. (*Continued*).

pulse-shape discrimination (PSD). PSD permits rejection of gamma photon-based detector counts from those caused from neutron interactions. At the PSD settings used for the published studies (Taleyarkhan et al., 2002, 2004, 2006a,b; Xu et al., 2005; Forringer et al., 2006a,b) it is estimated that roughly 95% of gamma photons are rejected. Fig. 2a shows the relative spectral emissions for each of these three emission types. Results of the measurements for each of these three sources with and without PSD are shown in Fig. 2b. As noted from Fig. 2b, the monoenergetic 14.1 MeV neutron spectrum displays a sharp reduction in counts at the 14.1 MeV PRE region (channel ~175) but counts still persist and leak into higher channels due to imperfect detector resolution. Since a 14.1 MeV D–T accelerator does not generate gamma photons, the vast majority of counts are neutron driven. For a Pu–Be source, as noted from Fig. 2a, the neutron energies are not monoenergetic but spread out over a large range (0.1 MeV–~10 MeV; the average energy is in the 4 MeV range with a tail towards 11 MeV at which the intensity drops close to zero. Importantly, a Pu–Be source also emits a strong 4.4 MeV gamma photon (Knolls, 1999), roughly at the same rate as for neutron emission; however, unlike the neutrons which are spread out in energy, the gamma photon is monoenergetic due to which, per expectations, we note in Fig. 2b a noticeable jump in the combined neutron-gamma (i.e., without PSD) spectrum around channel 90. As is also seen from Fig. 2a, for the ^{252}Cf isotope-based source, the neutrons are emitted from spontaneous fission with a peak intensity at ~0.8 MeV, with an average spectrum energy of ~1.98 MeV, and with a long tail extending through ~12 MeV where the intensity drops close to zero. ^{252}Cf also emits about three times more

Author's personal copy

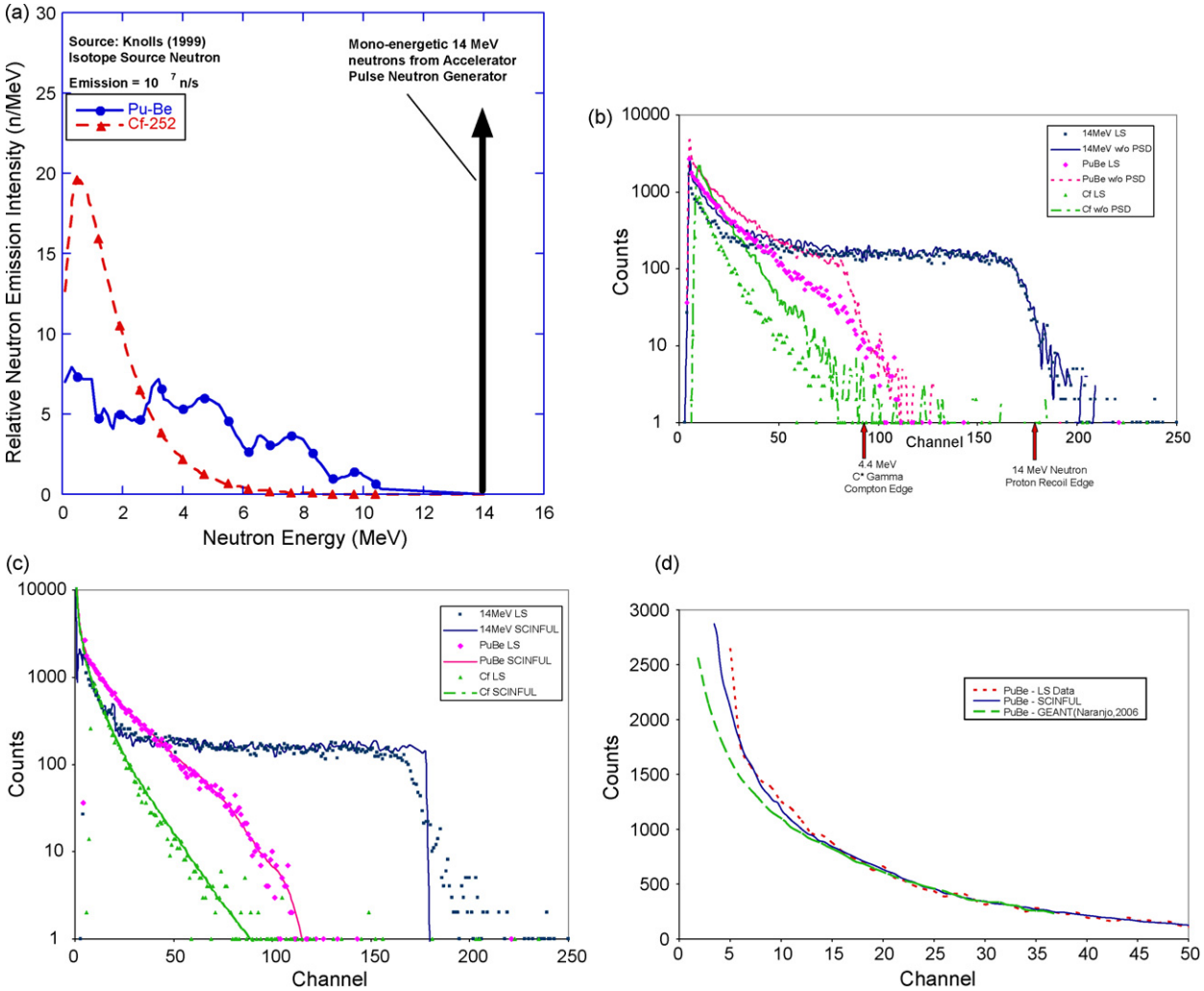

Fig. 2. (a) Spectral shapes of neutron emission intensity vs. energy for various sources used for calibration studies. (b) Measured pulse-height neutron-gamma spectra using 5 cm × 5 cm NE-213 LS Detector with (symbols) and without (lines) pulse-shape-discrimination (PSD) with isotope (^{252}Cf, Pu–Be) and 14 MeV mononergetic neutron from PNG. (c) SCINFUL Code predictions vs. measured neutron spectra with 5 cm × 5 cm NE-213 LS detector (with PSD). (d) SCINFUL and GEANT code predictions vs. measured neutron spectrum from a Pu–Be neutron source using a 5 cm × 5 cm NE-213 LS Detector. *Note*: Under predictions at lower channels are more pronounced for GEANT calculations—a feature which has also been reported by Patronis et al. (2007).

gamma photons (Knolls, 1999) for each neutron emission and we see this in the measured spectrum of Fig. 2b.

The 14.1 MeV neutron energy and published neutron spectra for the ^{252}Cf and Pu–Be sources were entered as input for SCINFUL code predictions of response for a 5 cm × 5 cm NE-213 detector. This is similar to what one would undertake to do if one were to rely on simulations (e.g., from MCNP5 predictions of down scattered neutron spectra). Results of SCINFUL code predictions for each of the three neutron sources are shown in Fig. 2c alongside the measured LS detector spectra with PSD. As noted therein, the SCINFUL code predictions capture the overall neutron spectral shapes for all three sources with excellent correlation over the entire energy range of ~0.5 MeV at the lower-level cutoff, to ~14 MeV, for the monoenergetic 14.1 MeV neutron spectrum. The coefficient for determination (so-called $R^2 = 1 - SS_{err}/SS_{tot}$; where SS_{err} is the regression sum of squares, and SS_{tot} is the total sum of squares proportional to the sample variance) ranged from ~91% to ~98%. Around the PRE channel (~175) SCINFUL predicts a sharp (almost vertical) rise in counts indicating the response to a head-on collision of the 14.1 MeV neutron with protons in the LS detector liquid. The measured spectrum also shows a significant rise in counts but the shape of this measured spectrum is somewhat smeared as expected for practical detectors (i.e., slanted at ~45° with counts leaking through to channel 250). Such an effect is well-known (Dickens, 1988; Knolls, 1999; Lee and Lee, 1998). This calibration-cum-benchmarking provides good confidence in the ability to predict the spectral response of a 5 cm × 5 cm NE-213 LS detector using a combination of an arbitrary input spectrum of neutron energies together with the SCINFUL code.

At the lower end of the abscissa corresponding to low-angle scattering of neutrons with protons and carbon atoms, a discrepancy between prediction and measurements may be expected as shown in Fig. 2d for comparisons against the measured Pu–Be neutron source spectrum of Fig. 2a. Also presented in Fig. 2d is the published prediction for a Pu–Be source using another Monte-Carlo based code, viz., GEANT (Agostinelli et al., 2003; Naranjo, 2006). SCINFUL and GEANT both tend to somewhat under predict the measured spectrum with the under prediction being greater for the GEANT code simulation as has also been reported elsewhere in the literature for GEANT (Patronis et al., 2007). However, except for some under prediction at lower channels, for most of the energy scale through the PRE channels and beyond, both SCINFUL and GEANT appear to be well-suited for predicting the measured neutron response spectrum for the NE-213 LS detector.

Author's personal copy

It is also well-known and documented for the SCINFUL code (Dickens, 1988) that detector resolution will vary from detector to detector depending on numerous factors such as light collection efficiency at liquid–photomultiplier interface, age of the detector, etc. Models of detector response for neutron-induced proton recoils therefore, usually model the detector as being one of perfect resolution—which then leads to a sharp increase at the PRE and no counts beyond the PRE (whereas, in actuality a sloping shoulder will be present and counts will occur in channels far beyond the PRE channel number). The capturing of such an effect is at times attempted by Monte-Carlo codes by artificially including a so-called resolution function (see for example, Dickens, 1988) for a given practical detector to force-fit the code predictions at the PRE location to the actual data profile against which it is to be compared in the first instance. Nevertheless, even without engaging in such artifacts, as also demonstrated with our own calibration in this section, the combined MCNP5–SCINFUL code system offers an excellent tool for predicting and studying the essential characteristics of the expected pulse-height spectrum for our experiments for the bulk of the pulse-height spectrum (i.e., for channels below the PRE).

3. Modeling approaches for comparing predictions with measured spectra from acoustic inertial confinement (bubble) fusion experiments

The calibrated SCINFUL code approach which was just discussed was next used to predict the LS detector neutron pulse-height spectrum for comparison against the published spectra. However, instead of using the well-established (i.e., known) neutron energy and spectrum of neutrons from an isotopic or PNG source, the neutron energy spectrum has now to be calculated. A D–D thermonuclear fusion event produces a 2.45 MeV neutron. In a typical bubble fusion experiment, this 2.45 MeV neutron is produced within a deuterated liquid contained in a test cell of approximately 3 cm in radius. Before reaching the LS detector this fusion neutron would necessarily become down scattered in energy as it interacts with intervening atoms of the test liquid, the container wall and shielding materials. It is this downscattered neutron energy spectrum which becomes the source input for SCINFUL predictions of the LS detector pulse-height response, which thereafter, can be directly compared against published experimental data to note how well the published spectra compare with the predicted values. Good agreement provides validation for the neutron source as being that from a D–D fusion event, in much the same manner as the good agreements of Fig. 2c validated the source of neutrons as being from ^{252}Cf, Pu–Be and PNG neutron sources, respectively.

3.1. MCNP5–SCINFUL response simulation

Therefore, as a first step, the transport characteristics of a 2.45 MeV neutron through ~3 cm of test cell liquid, followed by the enclosure wall, were computed using the well-known MCNP5 nuclear transport code (MCNP, 2003) developed by the Los Alamos National Laboratory (LANL). A three-dimensional (3D) model for each of the experimental geometries shown in Fig. 1 was developed. The prediction of the emanated spectrum was used as input for SCINFUL predictions as done before in Section 2. This calculational model is referred to as MCNP5–SCINFUL.

3.2. MCNP5–NE-213 response simulation—an alternate independent approach (MCNP5 neutron spectrum combined piece-wise with measured NE-213 detector response for various neutron energies)

A second modeling approach (refered to herein as "MCNP5–NE-213") was developed to independently compare with the

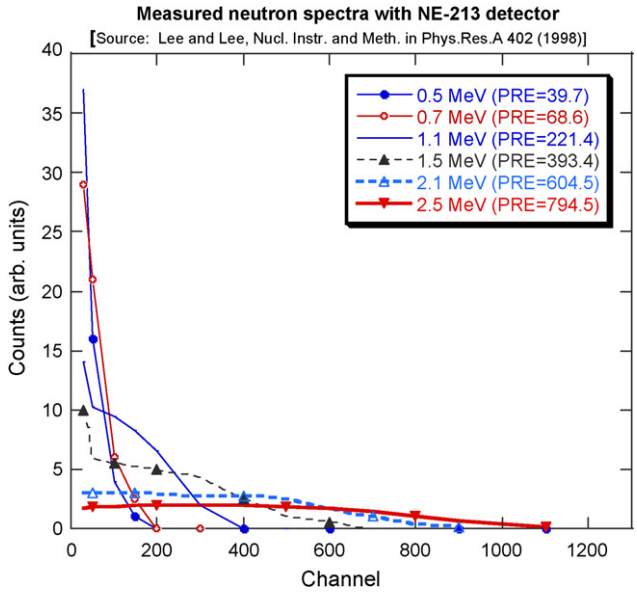

Fig. 3. Measured pulse-height spectra in a 5 cm × 5 cm NE-213 detector (Lee and Lee, 1998) for neutron energies ranging from 0.5 to 2.5 MeV. *Note*: The PRE channel was chosen to be mid-way of the shoulder for each curve (e.g., for 2.5 MeV, the PRE light output channel was deemed to be ~800). Note also that, due to imperfect detector resolution, significant counts occur above the PRE channel.

predictions of the MCNP5–SCINFUL code predictions discussed earlier. This was considered useful for two reasons. First, to cross-check and evaluate that SCINFUL code predictions against experimental data were in line with expectations for the spectrum shape below the 2.45 MeV PRE. The second reason was to help assess how many and how far above the 2.45 MeV PRE one should expect counts due to imperfect detector resolution, a well-known effect (e.g., Dickens, 1988; Lee and Lee, 1998) and also highlighted in established textbooks on the subject (Knolls, 1999). Fortunately, in a relevant study (Lee and Lee, 1998) the authors used a 5 cm × 5 cm NE-213 detector identical in size to the one used in the Taleyarkhan et al. (2002, 2004, 2006a,b), Forringer et al. (2006a,b), and Xu et al. (2005) studies. The Lee and Lee study has published individual pulse-height spectra at six neutron energies ranging from 0.5 MeV to 2.5 MeV. Their results of the measured spectra are replotted in Fig. 3, where the legend for each neutron energy includes the PRE channel number for each of the six neutron energies. As also noted from standard textbooks (Knolls, 1999) we readily note that significant counts can be expected in channel numbers far above the PRE channel for NE-213 type LS detectors. The availability of the six profiles at various neutron energies permits one to combine MCNP5 predictions for incoming neutrons at various energies with these six profiles, thereby acting as a cross-check for the *MCNP5–SCINFUL* model. That is, instead of relying solely on SCINFUL, we can now also rely on the published experimental response curves at discrete neutron energies of Fig. 3 for an actual detector of the type and size used in the bubble fusion experiments of Taleyarkhan et al. (2002, 2004, 2006a,b), Xu et al. (2005), and Forringer et al. (2006a,b). This model is herein, referred to as the MCNP5–NE-213 model.

However, since MCNP5 predictions for down scattered neutrons are over a continuous energy range, the MCNP5–NE-213 model requires binning. For this reason, the MCNP5 neutron spectrum variation with energy is broken down into six energy groups consistent with the six neutron energies of Fig. 3 to provide the relative proportion of neutrons in each bin. Thereafter, the digitized values of pulse-height spectra of Fig. 3 at each of six energy levels are multiplied by the relative fractional neutron counts (from MCNP5

Author's personal copy

simulations) in corresponding energy bins and the individual spectra are combined to obtain an overall composite spectrum.

4. Comparison of MCNP5–SCINFUL and MCNP5–NE-213 predictions with self-nucleation and externally nucleated bubble fusion experimental data

Comparison of predictions is shown separately for the self-nucleation experiments and then for the external neutron-based bubble fusion experiments. The more recent self-nucleation experiments are addressed first.

4.1. Comparison with self-nucleated bubble fusion experimental data

In self-nucleated bubble fusion experiments of Taleyarkhan et al. (2006a,b) and Forringer et al. (2006a,b) and Bugg (2006), the nucleation of bubbles was achieved using dissolved uranyl nitrate (a radioactive compound). The test cell and deuterated mixture-cum-uranyl nitrate (UN) contents were modeled using MCNP5 to represent the physical systems described in published documents (Taleyarkhan et al., 2006a; Forringer et al., 2006a,b). 2.45 MeV neutrons were sourced into the middle of the test cell fluid and the transport characteristics through the test liquid, glass walls, and experiment enclosure was assessed using the Monte-Carlo method. The actual experimental geometry also included a layer (~5 cm thick) of paraffin blocks on three sides, and for one side of the enclosure for the experimental configurations of Taleyarkhan et al. (2006a) and of Forringer et al. (2006a,b), respectively. The paraffin blocks served as biological shielding material for experimenters. Fig. 4 displays representative results for the down-scattered neutron energy spectrum in terms of fraction of the total at the NE-213 LS detector face with and without the presence of the 3 cm thick ice-pack material. It is readily seen that the original 2.45 MeV neutron experiences significant down scattering resulting in a range of neutron energies down to thermal energy levels. The extent of down scattering is enhanced significantly with the addition of 3 cm of water (ice-pack) shielding. The displayed results have included all neutrons from 0 MeV to 0.1 MeV in a single energy bin, which accounts for the significantly larger counts for the first energy bin.

The resulting neutron energy spectrum was then used in conjunction with the SCINFUL code for modeling the response of

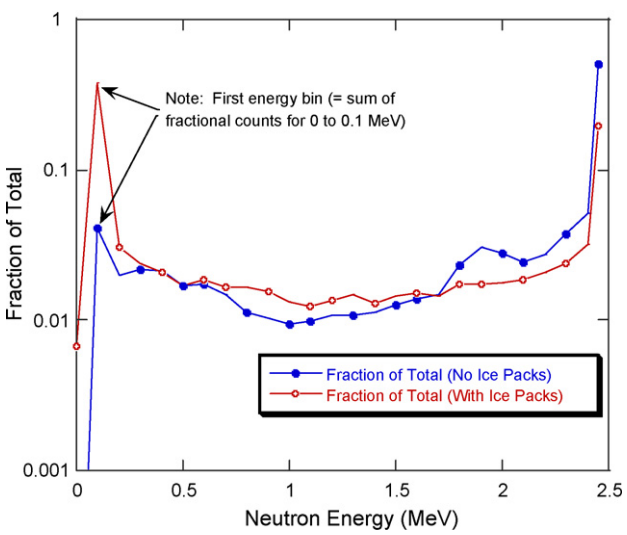

Fig. 4. MCNP5 computed neutron energy distribution for 2.45 MeV neutron after transport through 4 cm of test cell contents and then through 3 cm of ice-pack (modeled as water).

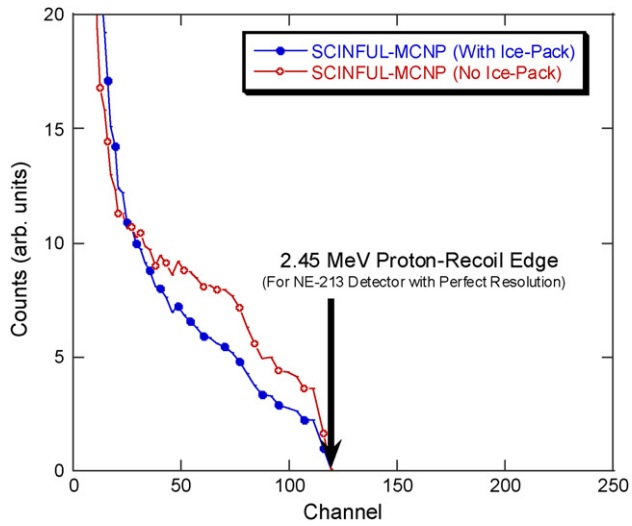

Fig. 5. Monte-Carlo simulation (SCINFUL-MCNP5) prediction of counts vs. light-output (pulse-height) for bubble fusion neutron spectra of Fig. 2 with and without ice-pack shielding.

NE-213 LS detectors to obtain the emanating light pulse-height response spectrum. In so doing, the MCNP5 predicted values for emitted neutron emission spectra of the type shown in Fig. 4 were utilized as inputs for the SCINFUL code to then derive the neutron spectral shapes (Fig. 5) with and without ice-pack shielding. Clearly the spectrum with ice-pack thermal shielding is noticeably different from the spectrum without ice-pack shielding and underscores the importance of accurately including intervening shielding materials. With the ice-pack materials included one notices a largely hyperbolic-like profile (reminiscent of the spectrum from a Cf-252 isotopic neutron source); without ice-pack shielding, the spectrum shape exhibits an anticipated hump starting from the PRE channel region.

Whereas, the spectrum with ice-packs appears qualitatively similar to that measured by Taleyarkhan et al. (as published in Fig. 4 of Taleyarkhan et al., 2006a,b), the calculated light output pulse-height spectrum without ice-pack shielding approximates the general characteristics of the spectrum measured by Forringer et al. (2006a,b), and by Taleyarkhan et al. (2004) and also to the spectrum calculated at UCLA (Naranjo, 2006) where the ice-pack thermal shield material was not included in the computational model. A more comprehensive comparison of data and predictions is provided below.

Next, the MCNP5–NE-213 model was used in which the MCNP5 results (Fig. 4) were binned and combined with the NE-213 LS detector response curves to arrive at the net response spectra of an LS detector for D–D fusion events within the test cell. As done for the MCNP5–SCINFUL model, results were obtained for the two cases with and without ice-pack shielding.

Results from the two approaches can now be compared against the Taleyarkhan et al. (2006a,b) measured neutron spectrum and the various results are shown in Fig. 6 for the experimental case (i.e., with ice-pack shielding). The corresponding results without ice-pack shielding are compared with the experimental measurements of Forringer et al. (2006a,b) as shown in Fig. 7. The reported UCLA predictions using GEANT (Naranjo, 2006) which were conducted without inclusion of intervening ice-pack shielding are also included in Fig. 7. We can now make the following observations:

(i) Ref. Fig. 6: When ice-pack shielding is taken into account, the MCNP5–SCINFUL as well as the MCNP5–NE-213 predictions for

Author's personal copy

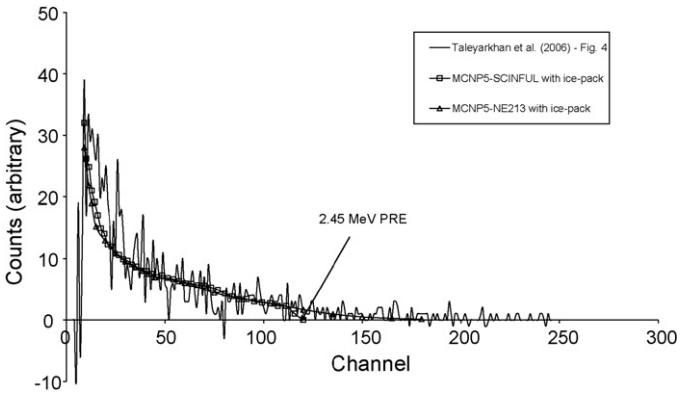

Fig. 6. Predictions of MCNP5–SCINFUL and MCNP5–NE-213 (Lee/Lee) methods vs. measured neutron response spectrum of Taleyarkhan et al. (2006a,b); with ice-pack shielding.

the measured neutron spectrum are consistent with and compare very well with the measured and reported bubble fusion neutron spectrum (Taleyarkhan et al., 2006a,b). For this comparison, the Taleyarkhan et al. measured results at Channel 50 were scaled to equal the predicted value of counts from the MCNP5 based predictions (at the same channel), after which the same scale factor was used for all other channels.

(ii) Ref. Fig. 6: Both MCNP5–SCINFUL and MCNP5–NE-213 predictions are consistent with each other below the 2.45 MeV PRE. Above the 2.45 MeV PRE, the MCNP5–SCINFUL model predicts no counts as would be expected. However, the MCNP5–NE-213 model's detector data-weighted predictions extend ∼50 neutron channels above the 2.45 MeV PRE. This is a further confirmation that real-life detectors, with imperfect resolution characteristics, should be expected to allow neutron counts to be collected above the PRE channel. It also provides an important and independent corroboration for, and a valid reason for the excess counts measured (above the PRE) in the neutron spectrum during bubble fusion experiments (Taleyarkhan et al., 2006a,b).

(iii) Ref. Fig. 7: The MCNP5–NE-213 approach which is based on actual measurements offers results which are consistent with the MCNP5–SCINFUL and the public-source GEANT code predictions of UCLA. All three approaches are reasonably close to each other and consistent in terms of overall shape and quantity of counts to be expected below the 2.45 MeV PRE.

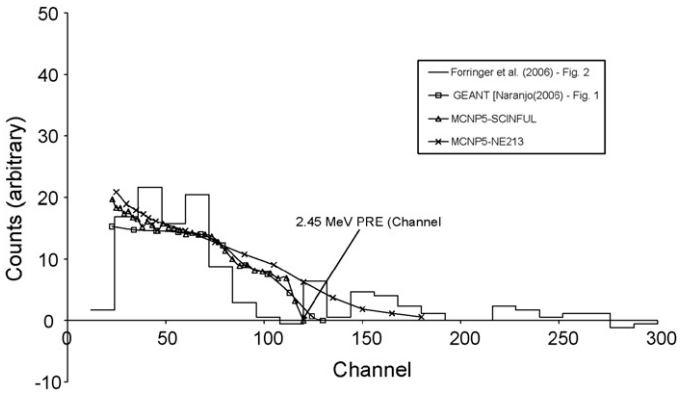

Fig. 7. Predictions of MCNP5–SCINFUL and MCNP5–NE-213 (Lee/Lee) methods vs. measured neutron response spectrum of Forringer et al. (2006a,b) for no ice-pack shielding and scaled GEANT code predictions from Naranjo (2006).

(iv) Ref. Fig. 7: The published bubble fusion neutron spectrum of Forringer et al. (2006a,b) which were obtained without intervening ice-pack shielding is consistent with and compares well with all three prediction schemes. The bubble fusion spectrum of Taleyarkhan et al. (2006a,b), and Forringer et al. (2006a,b) measurements both show counts above the 2.45 MeV PRE and this is also confirmed and predicted by using the MCNP5–NE-213 method.

4.2. Comparison with external neutron nucleated bubble fusion experiments using deuterated acetone

We next turn attention to the earlier bubble fusion experiments of Xu et al. (2005) and Taleyarkhan et al. (2002, 2004). Both of these experimental studies were conducted using pure deuterated acetone as the test liquid. A key difference was that the Xu et al. experiments were seeded with randomly emitted neutrons of various energies from an isotopic neutron source, whereas, the Taleyarkhan et al. studies were conducted using 14 MeV monoenergetic neutrons from an accelerator. Another major difference involved the presence of ∼3–4 cm of ice buildup at the freezer walls between the test cell and the LS detector for the Xu et al. (2005) studies, as shown schematically in Fig. 1c, whereas, there was no such intervening ice for the geometry (Fig. 1d) for the Taleyarkhan et al. (2002, 2004) studies.

4.2.1. Comparison against the external neutron nucleated bubble fusion experiments of Xu et al. (2005)

MCNP5 modeling and analysis was conducted for the general geometry of the Xu et al. (2005) studies. Results of the downscattered 2.45 MeV neutrons for various amounts of ice-buildup are shown in Fig. 8a. Fig. 8b presents the variation of fractional down scattering of 2.45 MeV neutrons emitted from the test cell with ice thickness, and one notices the expected exponential-like trend. In Fig. 8a and b we note that due to the exponential downscattering behavior of neutron transport, errors in the actual ice buildup around the nominal 3 cm (∼1 in.) value can be expected to remain small. As such, MCNP5–SCINFUL and MCNP5–NE-213 model simulations for the LS Detector response were conducted assuming the ice-buildup thickness of 3 cm.

Results of neutron pulse-height spectra are shown alongside the measured (published) data of Xu et al. (2005) in Fig. 9. It is clearly seen that, over the vast majority of the pulse-height spectrum the comparisons of the MCNP5–SCINFUL as well as MCNP5–NE-213 models are in very good agreement with the data.

4.2.2. Comparison against external neutron nucleated bubble fusion experiments of Taleyarkhan et al. (2002, 2004)

A scoping attempt was also made to compare predictions of the modeling approach against the data obtained with 14.1 MeV externally nucleated bubble fusion experiments of Taleyarkhan et al. (2002, 2004). For the geometry of this experiment shown in Fig. 1d, there was no intervening ice-packing material between the test cell and the LS detector. Due to this aspect one would expect a sharp bump of counts around the 2.45 MeV PRE channel. A complexity arises due to the use of 14.1 MeV neutrons from the PNG for nucleating bubbles. The 14.1 MeV neutron results in a significantly high background due to which, excess counts due to 2.45 MeV neutrons emanating from the test cell, and which are above the 2.45 MeV PRE channel cannot be statistically discriminated from the large 14.1 MeV related background counts. Nevertheless, to decipher first-order effects, MCNP5 was used to model the test cell and detector alone surrounded by the ice-pack walls as shown in Fig. 1d. Due to this aspect, some discrepancies may be expected for the profile of the downscattered neutron energies reaching the LS

Author's personal copy

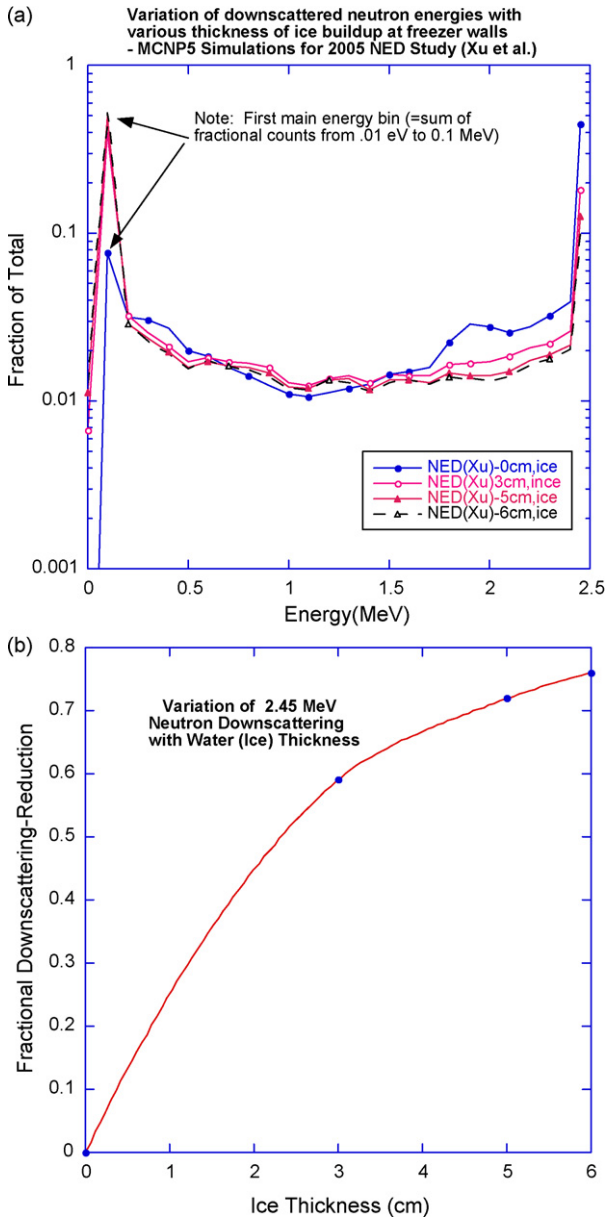

Fig. 8. (a) MCNP5 model predictions for variation of downscattered neutron energies for various thicknesses of ice buildup at freezer walls for externally nucleated experiments of Xu et al. (2005) with deuterated acetone. (b) Variation of fractional downscattering of 2.45 MeV neutrons with ice-thickness for Xu et al. experimental geometry (2005).

detector at the lower channels. Nevertheless, we were mainly interested to note if the principal trends from the MCNP5–SCINFUL and MCNP5–NE-213 model predictions are in general agreement with the published data of Taleyarkhan et al. (2004). Fig. 10 shows the MCNP5 results of downscattered neutrons at the LS detector volume for the geometry of Fig. 1d. Fig. 11 shows the MCNP5–SCINFUL and MCNP5–NE-213 model predictions versus the measurements. The comparisons indeed confirm that the overall trend is well-predicted. The measured spectrum is consistent with that of a 2.45 MeV neutron emitted from a D–D fusion event from within the test cell. In stark contrast to the comparisons against data taken with intervening ice-pack shielding (Fig. 9), when ice-packing is absent, we note a sharp bump in counts around the 2.45 MeV PRE channel in both the MCNP5–SCINFUL model predictions as well as for the measured spectrum of Taleyarkhan et al. (2004).

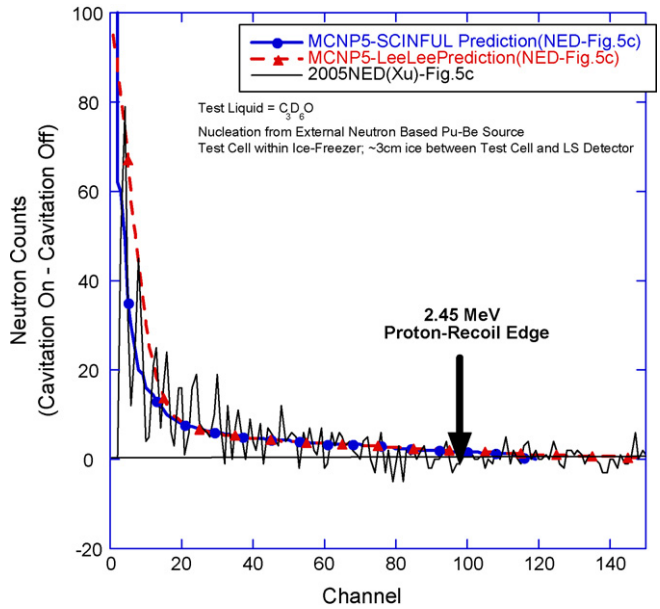

Fig. 9. Predictions of MCNP5–SCINFUL and MCNP5–NE-213 (Lee/Lee) models vs. measured neutron response spectrum (cavitation on–cavitation off) of Xu et al. (2005; Fig. 5c) with ice-pack shielding for external neutron nucleated fusion experiments with deuterated acetone.

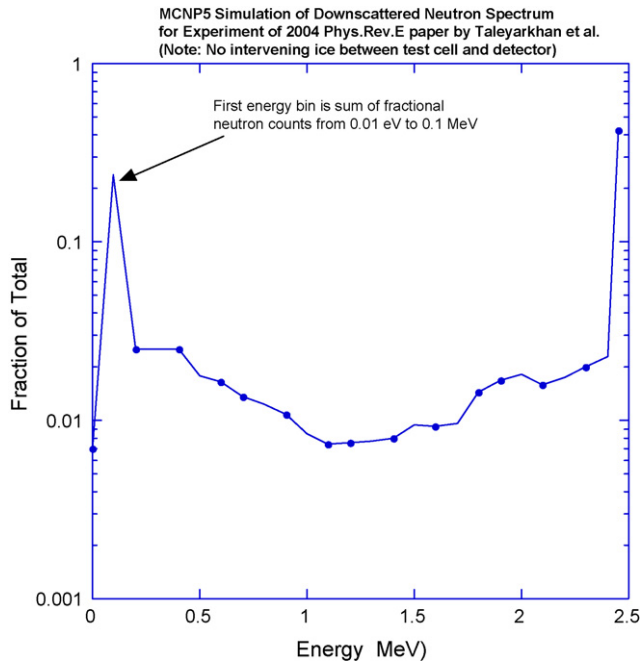

Fig. 10. MCNP5 predictions of down-scattered 2.45 MeV neutrons for Taleyarkhan et al. (2004) with 14 MeV PNG externally nucleated bubble fusion experiments.

5. Experiments and analyses to address the source of measured counts above the 2.45 MeV proton recoil edge (PRE) for bubble fusion

In this section we provide observations and additional experimental data in relation to addressing the excess ("excess" means the additional counts above those from control experiments) counts that are seen above the 2.45 MeV PRE during our bubble fusion experiments using an NE-213 type LS detector. Overall, we have noted that up to ~95% of total excess neutron-gated counts are

Author's personal copy

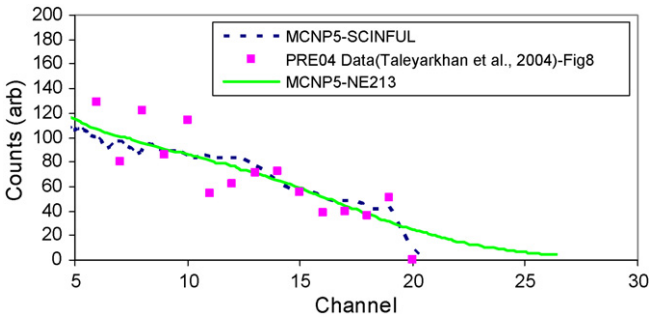

Fig. 11. MCNP5–SCINFUL and MCNP5–NE-213 model predictions vs. excerpted experimental data of Taleyarkhan et al. (2004; i.e., difference of counts from cavitation on minus cavitation off from Fig. 8c) with 14 MeV PNG externally nucleated bubble fusion experiments. *Note*: Counts above the 2.45 MeV PRE channel #21 are difficult to distinguish due to the large 14 MeV neutron background counts of about ~70–80 counts per channel.

obtained below the 2.45 MeV PRE. We have already covered one reason as being due to LS detector resolution, but other factors may also play a role. The source of additional counts above the 2.45 MeV PRE for the LS detector based results are believed to be due to the following phenomena.

5.1. Finite detector resolution

Due to finite detector resolution, the 2.45 MeV PRE turns away from being a sharp rise at the maximum proton recoil energy of 2.45 MeV to a smeared shoulder (Knolls, 1999; Lee and Lee, 1998; Dickens, 1988) as already shown in the previous plots, Figs. 2–7. We estimate the spread to be in the range of up to ~50% light channels above the designated PRE. For our published bubble fusion data during self-nucleated acoustic cavitation, much of the excess counts above the 2.45 MeV PRE will occur within ~50 channels of the PRE channel number. However, beyond the first ~50 channels over the PRE, the finite resolution feature in itself cannot answer why excess counts appear in higher channels and as such, other potential contributors need to be evaluated.

5.2. Imperfect PSD-related γ leakage into the neutron window

In our 1/2006 PRL manuscript (Taleyarkhan et al., 2006a,b), we have pointed out that the PSD system settings were ~93% efficient in terms of gating out gamma photons. This implies that about 7% of gamma photons produced during bubble fusion will necessarily leak into the neutron window. For the geometry of the setup (Fig. 1 of Taleyarkhan et al., 2006a,b), the test cell was enclosed within ice-pack filled enclosure and in addition, there was significant paraffin biological shielding blocks in the vicinity. Neutrons produced from fusion would first downscatter, then interact with Cl atoms in the test liquid to produce ~1.0 MeV to ~1.5 MeV photons, but ultimately, with the abundance of hydrogen atoms around, neutron capture can also result in 2.2 MeV gamma photons. The light pulse-height from 2.2 MeV gamma photons encompasses the entire channel range of the multi-channel analyzer (MCA). Therefore, gamma photons could be readily counted above the 2.45 MeV PRE. As an estimate, using a NaI detector we had reported (Taleyarkhan et al., 2006a) an excess gamma photon count rate of ~0.55 γ/s. A typical experiment lasting about 300 s would collect ~170 gamma photons, of which about 10% (~17) would be able to leak into the neutron window. From a typical excess neutron count population of about 1000 this amounts to about 1.5% of the total population.

5.3. Neutron and gamma counts from fission with uranium in the test cell liquid

For experiments involving self-nucleation using alpha-recoils from uranium decay, the fission of uranium from D–D fusion neutrons may also theoretically lead to counts above the 2.45 MeV PRE channel. The well-established nuclear industry's MCNP5 nuclear particle transport code [developed and maintained at Los Alamos National Laboratory (LANL)] was utilized to assess the neutron spectrum emitted from the test cell. As noted in Fig. 4, a significant fraction of the 2.45 MeV neutrons will be down scattered to lower energies before escaping from surface. About 5–8% of the neutrons were calculated to be scattered down in the energy range of 0–1 eV. Considering the relatively small number density of ^{235}U atoms and also ^{238}U atoms (for which the fast fission threshold is below 2.45 MeV) a preliminary estimate reveals a rather small («1%) fraction of the total excess neutron counts above the PRE that may result from fission. This phenomenon is not expected to be a significant contributor.

5.4. D–T fusion reactions, or ^{13}C–n interactions

The deuterated test liquid includes a small quantity of tritium, T (^{3}H) atoms and also a small fraction of the carbon, C atoms will be ^{13}C for which possibilities exist to produce nuclear fusion signatures. However, these contributions are assessed as being negligibly small. Only the D–T reaction may produce 14 MeV neutrons and as such, only a rare, occasional count may appear in the higher channels. The D–T reactions may occur as a result of T atoms being produced during D–D fusion as also from the trace (orders of magnitude lower than that for D atoms) concentrations of T atoms in the procured deuterated liquid itself.

5.5. Neutron pileup

A characteristic feature of acoustic inertial confinement (bubble) fusion is that the neutron emission is not continuous or random but implosion-based, and therefore, will be time-structured. Until recently, this aspect was not revealed as a possibility for excess neutron counts observed above the 2.45 MeV PRE. However, upon reconsideration and based on careful study of our recent theory paper published in the journal *Physics of Fluids* (Nigmatulin et al., 2005) new insights have been derived that appear to dictate that neutron pileup effects in LS detectors of the type used in the reported studies of Taleyarkhan et al. (2002, 2004, 2006a,b), Xu et al. (2005) and Forringer et al. (2006a,b) may indeed play a role in bubble fusion experiments. To further ascertain such an effect, we have conducted a series of experiments and analyses to quantify the relative contribution of neutron pileup (i.e., more than one neutron arriving at the detector within the detector's resolving time) during bubble fusion experimentation.

5.5.1. Experiments and analyses for neutron pileup effect during bubble fusion experiments

The theory of super-compression (Nigmatulin et al., 2005), as applied to our bubble fusion experimentation has revealed that the bubble implosion process leading to D–D fusion for a single bubble in a rapidly imploding cluster occurs within the time span of ~0.1 ps and it will emit about 12 neutrons per bubble implosion. The estimated bubble cluster consisting of ~1000 bubbles is calculated to involve about 40 to 50 bubbles within the interior of the cluster where the amplification in implosion intensity produces thermonuclear fusion conditions. There is some uncertainty involved in terms of estimating the time scale over which the 40–50 bubbles implode but conservatively, we estimate that

Author's personal copy

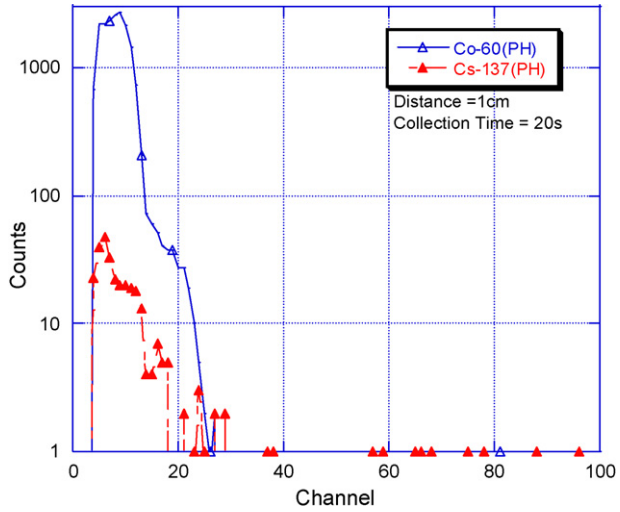

Fig. 12. Calibration spectra with ^{60}Co and ^{137}Cs.

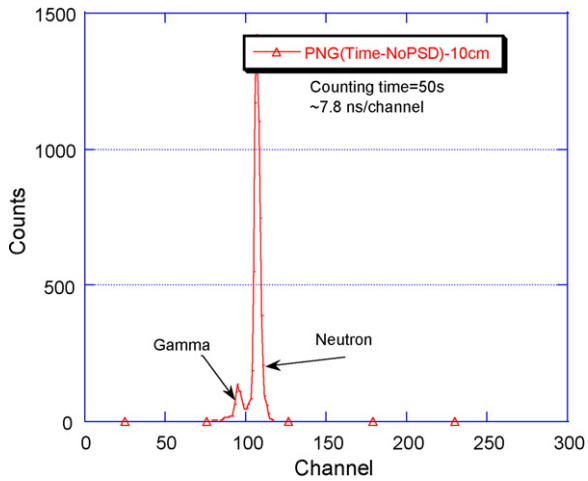

Fig. 13. Fusion (D–T) source PSD neutron-gamma spectrum with LS detector.

they collectively will implode over 100 ps emitting a total of about 200–400 neutrons. This gives us an estimate of the instantaneous rate of neutron emission of up to $\sim 4 \times 10^{12}$ n/s. This is a very high rate indeed and must be accounted for in terms of the possibility and consequence of more than one neutron arriving at the LS detector within the resolving (shaping) time of about ~100 ns (which is considerably longer than the much shorter emission period, which lies in the ps range).

The assessment of possible neutron pileup effects on our LS detector was conducted both with a pulsed neutron source and also via theoretical scoping analyses.

5.5.1.1. Experiments with a pulse neutron generator (PNG). We employed a D–T accelerator driven PNG (Model NN-550 from Activation Technologies, Inc.) for assessing whether neutron pileup effects could materialize in our LS detector for neutron pulse rates in the vicinity of expected bubble fusion neutron pulse rates. The PNG system enabled stable operation down to 200 Hz during which neutron pulses are emitted over a time span of ~5–6 μs (FWHM). The LS detector was placed with its face about 10 cm away from the PNG target. The LS detector response to ^{60}Co and ^{137}Cs sources was obtained. It was found (Fig. 12) that the ^{60}Co 1.2 MeV and 1.3 MeV gamma Compton edge is at channel ~15. From published light curves (Harvey and Hill, 1979) it would then imply that the 14.1 MeV PRE would appear around channel 105. With this calibration, the PSD spectrum was obtained and shown in Fig. 13. As previously noted, unlike that for an isotope-based neutron source, the D–T fusion based neutron source results in a much larger fraction of neutrons compared to gamma photons. D–T fusion does not produce gamma photons. Gamma photons are an indirect consequence of fusion neutron interactions with elements of surrounding structures. Based on calibrations with a 1 Ci Pu–Be source it was estimated that the PNG operating with a target voltage of −50 kV and 0.2 kHz would emit $\sim 5 \times 10^5$ n/s, close to the maximum emission level allowed in our laboratory. Since these neutrons are emitted in pulses (~10 μs wide at the base and ~5 μs FWHM) the instantaneous emission rate is much larger at $\sim 5\text{–}10 \times 10^8$ n/s ($=5 \times 10^5/5 \times 10^{-6}/200$). This formed a baseline for estimating the instantaneous pulse neutron outputs at other target voltages.

Next, neutron-gated pulse-height spectra were obtained at various target voltages ranging from −20 kV to −50 kV. Results of pulse-height spectra are shown in Fig. 14 along with the total neutron counts versus drive voltage in Fig. 15. As expected, the 14.1 MeV PRE is seen to occur around channel #105. The rate of neutron counts increase is more rapid at smaller target voltages and decreases as the target voltage increases. This is in line with well-known $\langle\sigma_v\rangle$ D–T reaction cross-sections (Gross, 1984). Fig. 14 clearly shows that, while insignificant excess counts are measured over the 14.1 MeV PRE at target voltages of less than −40 kV, the neutron pileup effect becomes noticeably larger for target voltage of −40 kV and above. The variation of the counts above the 14.1 MeV PRE with target voltage, expressed as a percentage is shown in Fig. 15. We see from Figs. 14 and 15 a rapid increase of neutron pileup induced counts above the PRE as the target voltage is increased.

The data shown in Fig. 14 were obtained with a source-to-detector distance of 10 cm compared with 30 cm in the published sonofusion experiments. This would imply a factor of ~10 [$=(30/10)^2$]difference based on solid angle effects, and to get about 3% of total counts above the PRE would require a rate of about 10^{11} n/s. This level of output at a distance of about 30 cm is comparable to (even though smaller than) the estimated $\sim 10^{12}$ n/s neutron emission rates for bubble fusion, thereby, forming a reasonable basis to expect that bubble fusion experiments with detection equipment of the type and configurations used will indeed lead to neutron-pileup related effects giving rise to excess counts above the PRE. The amount of excess may amount to ~5% of the total neutron counts.

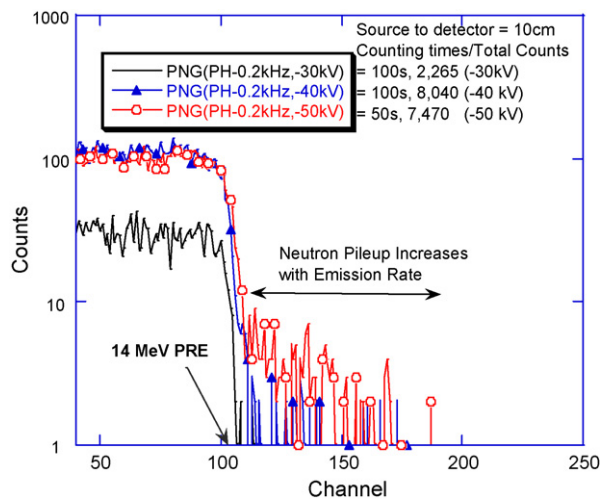

Fig. 14. Pulse-height spectra at various PNG target voltages (*Note*: −50 kV data were taken over 50 s not 100 s).

Author's personal copy

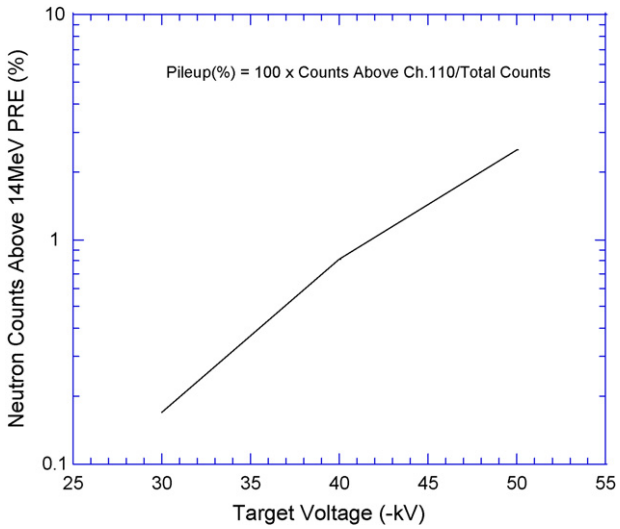

Fig. 15. Neutron pulse-pileup (%) vs. PNG target voltage.

5.5.1.2. Analytic estimation of magnitude of neutron pileup. If N neutrons are emitted during bubble cluster implosion such that they come within the resolving time of the detector, then the probability of a single neutron striking the detector is $N \times f$, where f is the fraction of the solid angle that the detector subtends.

The probability that two neutrons strike the same detector is $N(N-1)f^2$. If the detector efficiency is ε, then the net probability requires that we multiply by ε^2. The LS detector projects an area of about 25 cm^2 so that the solid angle "f" at 30 cm from the test cell becomes 0.0022. Since we have estimated that up to 500 neutrons are emitted per bubble cluster implosion, $N = 500$. Based on known scattering cross-sections for C and H atoms, and the composition of NE-213 liquid, for a 5 cm × 5 cm LS detector, the mean free path for a 2.45 MeV neutron is calculated to be ~5.3 cm. We can then assume that ~60% of all neutrons would receive at least one collision within the LS liquid, which then would offer a theoretical intrinsic efficiency of at least ~50%. Assuming a typical 50% detector (intrinsic) efficiency gives the net probability of the detector receiving two neutrons simultaneously = $500 \times 499 \times (0.0022)^2 \times (0.5)^2 = 0.3$ or about 30%. This methodology has assumed that each neutron regardless of energy striking the detector will contribute to the "pileup" effect equally. In reality, only neutrons above ~1.3 MeV would be able to have an effect. From MCNP5 assessments the fraction of neutrons above 1.3 MeV is estimated to be ~40% and ~80% with and without ice-pack thermal shielding, respectively. This reduction would bring down the above-estimated 30% down to ~20% [= 30% × $(0.8)^2$, without ice-packs] to ~5% [= 30% × $(0.4)^2$), with ice-packs], respectively. The approach of this section necessarily encompasses uncertainties, chiefly related to the value of "N", but on an overall basis, it appears in line with and on the order of magnitude of neutron pileup as also witnessed from the experimental observations.

Based on the above, it may be reasonably expected on theoretical grounds that neutron pileup could play an important role in terms of providing excess counts above the 2.5 MeV PRE and the amount to be expected may be in the experimentally observed range of up to ~5%–10% of the total neutron counts.

6. Summary and conclusions

In summary, a comprehensive framework has been developed to model, simulate and understand the 2.45 MeV neutron signature for acoustic inertial confinement (bubble) thermonuclear fusion signature. Both, self-nucleated and external neutron nucleated acoustic (bubble fusion) cavitation experiments have been modeled and analyzed for neutron spectral characteristics at the detector locations for all separate successful published bubble fusion studies. Monte-Carlo neutron transport calculations of 2.45 MeV neutrons from imploding bubbles were conducted, using the well-known MCNP5 transport code, for the published original experimental studies of Taleyarkhan et al. (2004, 2006a,b), as also the successful confirmation studies of Xu et al. (2005), Forringer et al. (2006a,b) and Bugg (2006). NE-213 LS detector response was calculated using the SCINFUL code. These were cross-checked using a separate and independent approach involving weighting and convoluting MCNP5 predictions with published experimentally measured NE-213 detector neutron response curves for monoenergetic neutrons at various energies. This resulted in the formulation of two models: (a) MCNP5–SCINFUL; (b) MCNP5–NE-213 models, respectfully.

The MCNP5-based model was first successfully calibrated and validated against experimental data with an NE-213 based LS detector for three distinct neutron sources: (a) ^{252}Cf; (b) Pu–Be; (c) 14.1 MeV neutrons from a PNG accelerator device. Excellent agreement was demonstrated versus actual experimental data for neutron spectra with PSD.

The impact of neutron pulse-pileup during bubble fusion was verified and estimated with a pulsed neutron generator based experiments and theoretical analyses, both of which provided confidence that an implosion-based bubble fusion process will likely lead to pulse-pileup in the LS detector train. This aspect is consistent with theoretical predictions from our theory paper on super-compression of deuterium atom vapor filled imploding bubbles. Other major contributions and reasons for measurement of nuclear counts above the 2.45 MeV PRE channel were shown to be due to imperfect LS detector resolution around the PRE, gamma photon leakage due to imperfect PSD. The impact of uranium fission and other effects such as D–T or ^{13}C–n reactions were estimated to be of low order in importance.

The MCNP5–SCINFUL and MCNP5–NE-213 models were employed to model and predict the neutron spectra from LS detectors for all of the published data involving both self-nucleation experiments (Taleyarkhan et al., 2006a; Forringer et al., 2006a,b) as well as earlier experiments conducted with external neutron based nucleation experiments (Taleyarkhan et al., 2002, 2004; Xu et al., 2005). A key determinant for the neutron spectral shape was shown to be related to the presence or absence of intervening ice-pack thermal shielding between the test cell and the LS detector. The self-nucleation experiments of Taleyarkhan et al. (2006a,b) and external neutron nucleated experiments of Xu et al. (2005) included the presence of ~3 cm of intervening ice-pack shielding between the LS detector and the test cell. However, the self-nucleated experiments of Forringer et al. (2006a,b) and the external neutron nucleated experiments of Taleyarkhan et al. (2002, 2004) did not include such intervening ice-pack shielding. All four experimental geometries were individually modeled using MCNP5 for deriving the transport characteristics of the 2.45 MeV fusion neutrons from within the test cell for each of the four experiments. The resulting neutron spectrum was next used to derive the LS detector spectral response using the MCNP5–SCINFUL and MCNP5–NE-213 models, respectfully.

The results of modeling-cum-experimentation were found to be consistent with published experimentally observed neutron spectra for 2.45 MeV neutron emissions during acoustic cavitation (bubble) fusion experimental conditions with and without ice-pack (thermal) shielding. Calculated neutron spectra with inclusion of ice-pack shielding are consistent with the published spectra from the experiments of Taleyarkhan et al. (2006a,b) and Xu et al. (2005)

Author's personal copy

where ice-pack shielding was present, whereas without ice-pack shielding the calculated neutron spectrum is consistent with the experimentally observed neutron spectrum of Taleyarkhan et al. (2002, 2004) and Forringer et al. (2006a,b). The reported GEANT code computer simulations of Naranjo (2006) were conducted with neglect of the intervening ice-pack shielding for the Taleyarkhan et al. (2006a,b) experiments. Since the Forringer et al. (2006a,b) study was conducted without intervening ice-pack shielding the published GEANT code simulation results were also compared against the Forringer et al. (2006a,b) reported spectrum. This comparison provided good overall agreement over the energy range of the reported data of Forringer et al. (2006a,b) and also with predictions from the MCNP5–SCINFUL and MCNP5–NE-213 model simulations.

The results of this manuscript confirm that the confusion and controversies caused from past reports (Reich, 2006; Naranjo, 2006) resulted from the neglect of important details and features of acoustic inertial confinement (bubble) nuclear fusion experiments and associated phenomenology.

Results from this paper demonstrate that ice-pack shielding between the detector and the fusion neutron source, gamma photon leakage and neutron pulse-pileup due to picosecond duration neutron pulse emission effects may play important role in affecting the spectra of 2.45 MeV D–D fusion neutrons from acoustic thermonuclear fusion experiments

Acknowledgments

This research was supported in part by Purdue University, State of Indiana, USA. Comments, and useful advice, careful review and critique were received from Dr. Colin West for improving the quality of the manuscript, and which are deeply appreciated and duly acknowledged. Editorial assistance and encouragement from Prof. G. Lohnert are gratefully acknowledged. Also gratefully acknowledged are USDoE's Radiation Safety Information Computational Center (RSICC) at Oak Ridge National Laboratory which supplied the simulation code systems MCNP5 and SCINFUL used for this study, as also Purdue University's radiological and environmental management systems (REMS) staff for their operations support. The LS NE-213 detector used in the reported studies was procured from Eljen Technology, Sweetwater, TX, which utilized EJ-301 as their trademark equivalent to the NE-213 scintillation liquid.

References

Agostinelli, S., et al., 2003. Nuclear Instrum. Methods Phys. Res. A 506, 250–303.
Bugg, W., 2006. Report on Activities on June 2006 Visit, Report to Purdue University, June 9, 2006.
Dickens, J.K., 1988. SCINFUL: A Monte Carlo Based Computer Program to Determine a Scintillator Full Energy Response to Neutron Detection for EN Between 0.1 and 80 MeV: User's Manual and FORTRAN Program Listing. ORNL-6462, United States Department of Energy's Radiation Safety Information Computational Center (RSICC) Report, PSR-267, Oak Ridge, TN, USA.
Forringer, E., et al., 2006a. Transactions of American Nuclear Society Conference, vol. 95, Albuquerque, NM, USA, November 15, 2006, p. 736.
Forringer, E., et al., 2006b. Proceedings of the International Conference on Fusion Energy, Albuquerque, NM, USA, November, 14, 2006.
Gross, R.A., 1984. Fusion Energy. John Wiley and Sons, Inc.
Harvey, J.A., Hill, N., 1979. Nuclear Instrum. Methods Phys. Res. 162, 507.
Knolls, G., 1999. Radiation Detection and Measurement. John Wiley and Sons.
Lee, J.H., Lee, C.S., 1998. Nuclear Instrum. Methods Phys. Res. A, 402.
Monte Carlo Team, 2003. MCNP—A General Monte Carlo N-Particle Transport Code, Version 5, vol. I: Overview and Theory. LANL Report LA-UR-03-1987. Los Alamos National Laboratory, Los Alamos, NM.
Naranjo, B., 2006. PRL 97 (October), 149403.
Nigmatulin, R.I., et al., 2005. Phys. Fluids 17, 107106.
Patronis, N., et al., 2007. Nuclear Instrum. Methods Phys. Res. A 578, 351–355.
Reich, E., 2006. Nature, 060306, news@nature.com (March 8).
Taleyarkhan, et al., 2002. Science 295, 1868.
Taleyarkhan, et al., 2004. Phys. Rev. E 69, 036109.
Taleyarkhan, et al., 2006a. PRL 96, 034301.
Taleyarkhan, et al., 2006b. PRL 97, 149404.
Xu, Y., et al., 2005. Nuclear Eng. Des. 235, 1317–1324.